Data Transparent and Polarization Insensitive All-Optical Switch Based on Fibers with Enhanced Nonlinearity

Matej KOMANEC, Pavel SKODA, Jan SISTEK, Tomas MARTAN

Department of Electromagnetic Field, Faculty of Electrical Engineering, Czech Technical University in Prague, Technicka 2, Prague 6, 166 27, Czech Republic

komanmat@fel.cvut.cz, skodapav@fel.cvut.cz, sistekj@fel.cvut.cz, martant@fel.cvut.cz

Abstract. *We have developed a data transparent optical packet switch prototype employing wavelength conversion based on four-wave mixing. The switch is composed of an electro-optical control unit and an all-optical switching segment. To achieve higher switching efficiencies, Ge-doped silica suspended-core and chalcogenide arsenic-selenide single-mode fibers were experimentally evaluated and compared to conventional highly-nonlinear fiber. Improved connectorization technology has been developed for Ge-doped suspended-core fiber, where we achieved connection losses of 0.9 dB. For the arsenic-selenide fiber we present a novel solid joint technology, with connection losses of only 0.25 dB, which is the lowest value presented up-to-date. Conversion efficiency of -13.7 dB was obtained for the highly-nonlinear fiber, which is in perfect correlation with previously published results and thus verifies the functionality of the prototype. Conversion efficiency of -16.1 dB was obtained with arsenic-selenide fiber length reduced to five meters within simulations, based on measurement results with a 26 m long component. Employment of such a short arsenic-selenide fiber segment allows significant broadening of the wavelength conversion spectral range due to possible neglection of dispersion.*

Keywords

All-optical networks, optical switching, wavelength conversion, four-wave mixing, chalcogenide fibers.

1. Introduction

Increasing data traffic such as 3D multimedia data streams, full-HD videos and real-time data transfers imposes demands for all-optical network solutions, represented by optical burst or optical packet switching. With the rise of new modulation formats in optical communication such as dual-polarization quadrature phase-shift keying (DP-QPSK) [1] and m-ary quadrature amplitude modulation (m-QAM) [1], [2], optical networks will require modulation format transparent, polarization insensitive switching processes with switching speeds in orders of Tbit/s. Several solutions to optical packet switching have been proposed, e.g. based on optical gating [3], optical flip-flops [4] or micro-electromechanical systems (MEMS) [5]. All-optical processing of a 4-bit optical packet label was presented in [6], where several RF signals were imprinted on each label.

Optical packet switching based on wavelength conversion offers a viable solution for future optical packet switched networks. The major advantage of wavelength conversion based on four-wave mixing (FWM) stands in modulation format and data bitrate insensitivity. Highly-nonlinear fibers (HNLFs) have been exploited for wavelength conversion [7]. Specialty non-silica and microstructured fibers, e.g., chalcogenide fibers [8], bismuth fibers [9] and microstructured fibers thereof [10], [11], provide extremely high nonlinearities (γ>1000 $W^{-1}km^{-1}$), promising enhanced conversion efficiencies while simultaneously decreasing component length, which can result in neglection of dispersive effects. Major drawback of these fiber stands in high coupling losses, when connected to a conventional silica fibers. Free-space optic approaches were proposed for coupling into arsenic-selenide fibers with only 37% coupling efficiency [12], but these are not suitable for real network application. Solid joints for arsenic-selenide fibers were presented [13] with 2.45 dB loss per joint achived by butt-coupling to silica fiber via 5 mm of high NA fiber and index matching oil to improve coupling. Furthermore in [13] arsenic-selenide single-mode fibers were measured and provided attenuation of $\approx$1 dB/m.

This paper presents results from the development of a prototype hybrid optical packet switch (OPS) based on optical fibers with enhanced nonlinearity (NLF) and electro-optical packet label processing. The aim was to provide transparent polarization insensitive data switching without exceeding the optical power limits in telecommunications ($\leq$ 23 dBm). For maximal OPS transparency, wavelength conversion based on FWM was exploited. Novel solid joint technologies were developed for chalcogenide fibers to enable efficient broadband wavelenght conversion. Polarization sensitivity was significantly decreased by employing a specific polarization insensitive configuration. Wavelength conversion efficiencies were measured for all NLFs, considering limiting effects and NLFs insertion loss.

The paper first discusses theory of the FWM effect and demands placed on the OPS and its functionality. Afterwards a prototype configuration for experimental evaluation is described. Wavelength range is evaluated and frequency plan is proposed for spectrally efficient optical packet switching. 10 Gbit/s non-return zero (NRZ) was measured experimentally and bit-error rate (BER) and optical signal-to-noise ratio (OSNR) tests were carried out. Optimization of the arsenic-selenide fiber is presented. The paper concludes with a summary of achieved results and future enhancement possibilities.

2. Theoretical Background

The FWM effect considers two co-propagating waves, often denoted as pumps, at frequencies ω_{p1} and ω_{p2}. If the phase-matching condition is fulfilled, both waves are co-polarized and nonlinearity of the medium is sufficient, two new signals emerge at difference frequencies, which are denoted as idlers. In case of degenerate FWM (DFWM) only one pump is present, i.e., the frequencies of the two pumps are identical $\omega_{p1} = \omega_{p2}$. Then the pump propagates in the medium and if a phase-matched, co-polarized signal (data) is present at ω_{data}, only one idler is generated at frequency ω_p - ω_{data}. DFWM is exploited mostly for wavelength conversion or parametric amplification. For this work DFWM will be discussed and utilized.

Conversion efficiency η is one of the main factors for wavelength conversion via DFWM, i.e., for optical data switching. It is fundamentally dependent on optical fiber nonlinearity, optical fiber length and utilized optical power (pump peak power) as [14]:

$$\eta = \frac{P_{switched}(L)}{P_{input}(0)} = \left[\frac{\gamma P_{pump}}{g}\sinh(gL)\right]^2 \tag{1}$$

and

$$\gamma = \frac{2\pi n_2}{\lambda A_{eff}} \tag{2}$$

where $P_{switched}$ stands for the switched data peak power, P_{input} is the input data peak power, γ stands for fiber nonlinearity, g is the gain coefficient, P_{pump} is the pump peak power, A_{eff} stands for the effective mode area, n_2 is the nonlinear refractive index and L represents NLF effective length.

It is obvious that higher nonlinear refractive index n_2, i.e. nonlinear coefficient γ, results in more efficient nonlinear processes. On the other hand higher values of n_2 are in correlation with refractive index n, which implies higher refractive index contrast. When connecting the nonlinear fiber to conventional silica fiber (which is sooner or later unavoidable in any OPS setup) connection losses are then implied. Second factor which is interconnected with n_2 is material attenuation, which increases with higher n_2. As a representative of NLF with high n_2) a chalcogenide arsenic-selenide single-mode fiber (As_2Se_3 fiber) was selected for our measurements.

Nonlinear coefficient γ depends (apart from n_2) on A_{eff} and λ, which was considered fixed in vicinity of 1550 nm (C-band), therefore only A_{eff} can be minimized to increase nonlinearity. To achieve A_{eff} decrease, microstructured optical fibers [11] or fiber tapering [15], [16] can be employed. Both these methods again imply increased component attenuation. As a representative of microstructured NLF a highly Ge-doped microstructured suspended-core single-mode fiber (Ge-SCF) was employed in our measurements.

Modulation format transparency is closely related to bitrate and polarization insensitivity, e.g. when DP-QPSK is applied, the signal is propagated in both polarization axes and is also phase modulated. Proposed switching methodology of FWM is able to convert advanced modulation formats. Attention was paid to selected formats utilized in current networks and recognized by the ITU-T and IEEE respectively [17], [18] – 10 Gbit/s NRZ, 40 Gbit/s DPSK and 100 Gbit/s DP-QPSK.

Polarization insensitivity is a crucial parameter for efficient DFWM, where high switching efficiency has to be ensured to reduce switched signal amplification requirements. Amplification of the switched data decreases its OSNR performance. Various polarization insensitive configurations for DFWM wavelength conversion are discussed and proposed in [19], [20], [21].

3. Experimental Setup

An experimental 1x2 switch protype setup is depicted in Fig. 1. The developed OPS consisted of four functional segments. The first segment was composed of a data payload generator, label generator and a multiplexer (MUX) forming the optical packet, whose length was designed to be 100 ns, with a 80 ns 8-bit long label. The second segment was responsible for input data buffering. The third segment detected and processed the packet label and governed routing signal generation. This was realized by an opto-electronic controller (OEC) with an embedded FPGA (field-programmable gateway array) controlled remotely via Ethernet. Afterwards the buffered input data was multiplexed with the routing signal in athermal arrayed-waveguide grating (AWG) specifically developed for the purpose of this prototype, with stable function from -40 °C to +80 °C. In the fourth section the coupled routing signals and input data propagated through NLF and a switched data payload (in this paper denoted as switched data) appeared at a new wavelength defined by the DFWM process. Then routing signals and input data were attenuated in an optical bandpass filter (OBF) and furthermore demultiplexed in AWG. New label was attached to the switched data at the output of AWG thus forming a new optical packet. Polarization insensitive configuration with NLF will be discussed in detail in a separate section.

Vizualization of the OPS prototype is depicted in Fig. 2, with output for amplifier attachment (front panel) and

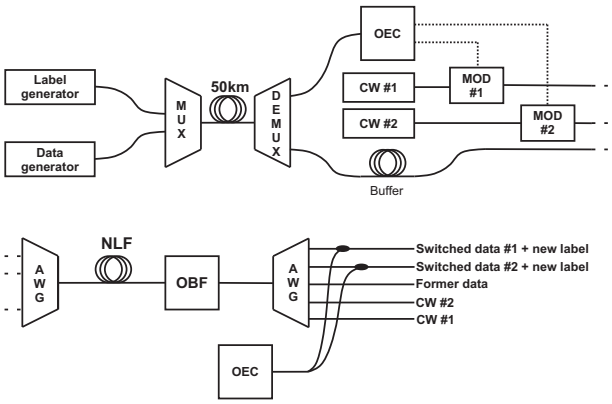

Fig. 1. Scheme of the proposed OPS setup, MOD – Mach-Zehnder modulator, MUX/DEMUX – multi/demultiplexer, PRBS – pseudo-random bit sequence, OEC – opto-electronic controller, NLF – fiber with enhanced nonlinearity, AWG – arrayed-waveguide grating.

Fig. 2. Optical packet switch prototype - visualization.

various nonlinear fiber testing (rear panel). The prototype can be operated in either manual or automatic regime and can be controlled via Ethernet.

A standard commercialy available HNLF was chosen as a representative of a conventional NLF. Fiber dimensions were similar to standard SMF-28e fiber, γ was measured to be 11.35 $W^{-1}km^{-1}$, zero-dispersion wavelength in vicinity of 1559 nm and attenuation of 0.7 dB/km. For the measurements a 500 m long component was employed.

A suspended-core microstructured silica fiber with highly Ge-doped core provided by IPHT, Jena, Germany was exploited with a core diameter of 6.6 μm, γ of 21.0 $W^{-1}km^{-1}$, dispersion D of 32.6 ps/nm/km at 1550 nm and attenuation of 43.0 dB/km. For experimental tests a 100 m component was exploited with connection losses of 0.9 dB per junction.

Chalcogenide As_2Se_3 single-mode fiber with single-mode cut-off at approximately $\sim$1300 nm, γ of approximately 1300 $W^{-1}km^{-1}$, dispersion D of -560 ps/nm/km at 1550 nm has been employed in our measurements. The fiber was prepared by the double-crucible technique developed at the Naval Research Laboratory [22]. It provided minimal core excentricity (below 1 μm), leading to simplified coupling to conventional fibers. A final component containing 26 m As_2Se_3 fiber spool with standard silica SMF-28e fibers at output was developed at SQS Fiber optics, Czech Republic. Insertion loss (IL) of 16.0 dB for the whole component was obtained. A study of backreflected power was performed, which provided evidence of reflection at the input As_2Se_3 connection, therefore we assume $\sim$0.25 dB loss per connection, which is the lowest loss according to authors knowledge for a As_2Se_3 single-mode fiber connection to conventional silica single-mode fiber reported world-wide up to date [13]. This leads to fiber attenuation of less than 0.6 dB/m (measured by the LUNA device), which is in contrast to manufacturer data of 0.72 dB/m at 1550 nm, furthermore this value is 0.4 dB lower than presented in [13]. It allows to develop As_2Se_3 components of $\sim$1 m lengths with insertion loss $<$1.5 dB, which is a significant result for further exploitation of nonlinear processes based on arsenic-selenide fibers.

Table 1 summarizes material losses α_{mat} and component measured insertion losses α_{comp} for employed fibers (with connection to standard SMF-28e fiber outputs).

Fiber	α_{mat} [dB/m]	α_{comp} [dB]
500 m HNLF	$7{\cdot}10^{-4}$	0.55
26 m As_2Se_3	0.580	16.00
100 m Ge-SCF	0.043	6.10

Tab. 1. Nonlinearity, material attenuation and component insertion loss.

4. Measurement

For initial comparison, all three evaluated NLFs were tested at +1 channel detuning of the input data from the pump signal (considering DWDM 100 GHz grid). The highest conversion efficiency was expected from HNLF as HNLF provided the most suitable combination of low component IL (0.55 dB) and γL coefficient of 5.67. Second highest from As_2Se_3 fiber and the lowest conversion efficiency was expected from Ge-SCF. As_2Se_3 fiber provided significantly higher γL coefficient of 33.8, but on the other hand component IL of 16.0 dB. Ge-SCF γL coefficient of 2.1 combined with component IL of 6.1 dB promised low conversion efficiencies. For all measurements the pump was tuned from 6 dBm to 16 dBm peak power, whereas the input data was kept at the same optical power.

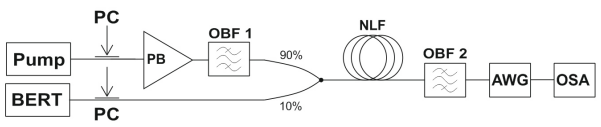

Fig. 3. Setup for conversion efficiency and wavelength range measurements.

Wavelength conversion efficiency η is independent of input data power (as defined in (1)), therefore only pump power played a critical role. In our case it was limited by the stimulated Brillouin scattering (SBS) effect (HNLF at 13.0 dBm, As_2Se_3 at 16.8 dBm and Ge-SCF at 26.6 dBm,

considering pump-width of 1 MHz). Employed thin-film components (e.g. multiplexer - MUX or AWG) are power limited at 23 dBm, which was significant only for Ge-SCF, as all other evaluated fibers had their SBS thresholds below the 23 dBm value. The pump phase-modulation technique to suppress SBS can be utilized to increase pump peak power, but if advanced modulation formats should be employed, phase-modulation of the pump severely decreases switched signal parameters, as is presented in detail in [23].

Measurement setup for conversion efficiency and wavelength range evaluation is presented in Fig. 3. A BER tester with a SFP module at 1552.52 nm serves as the data source, whereas a tunable laser source (ID Photonics CoBrite) provides the pump signal. Both are polarization controller (PC) and the pump is separately amplified in a power booster (PB) and excess noise is filtered in an optical bandpass filter (OBF 1). A 90/10 coupler is exploited to preserve pump power. After propagation through NLF the idler signal is filtered in another optical bandpass filter (OBF 2) and sent into an AWG. Output is monitored by an optical spectral analyzer (OSA) - Yokogawa AQ6370.

For all measurements the obtained spectra after the NLF are presented. Conversion efficiency is then calculated as the difference between signal power (before conversion, i.e. NLF) and idler power (after conversion, i.e. NLF). HNLF measurements are presented in Fig. 4 with conversion efficiencies better than -15 dB for pump peak powers over 13 dBm. This result is in correlation with previously published results at similar pump peak powers [24].

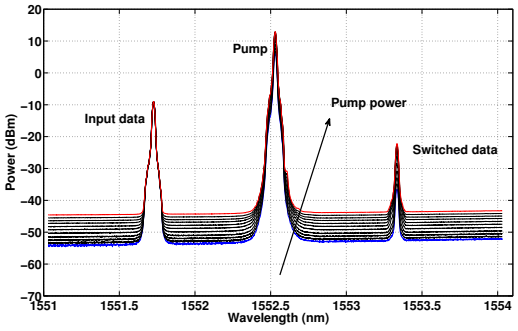

Fig. 4. Four-wave mixing in 500 m HNLF, pump power from 6 dBm to 16 dBm.

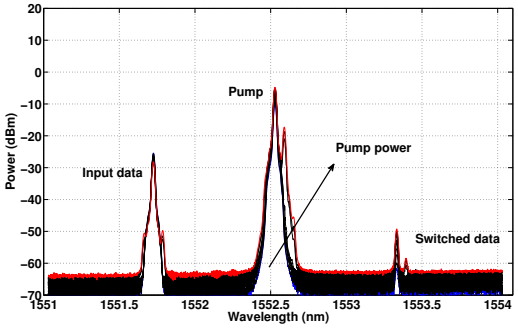

Fig. 5. Four-wave mixing in 26 m As_2Se_3 fiber, pump power from 6 dBm to 16 dBm.

Results for As_2Se_3 fiber are illustrated in Fig. 5. Chirped peaks appeared for the pump signal and the switched data payload. They were initiated by the reflection of the pump signal on the As_2Se_3/silica boundary and induced SBS on the reflected pump (in practice there was a conventional SBS backscattered signal and another SBS backscattered signal caused by the reflected pump, which then propagated in the same direction as the pump, data and idler). Conversion efficiencies were under -38 dB, where the major detrimental effect was implied by the component IL. As the effective length for sufficient nonlinear response of the As_2Se_3 fiber is 7.5 m, component IL reduction is possible to enhance nonlinear performance, therefore further simulations were carried out in Section 5.1.

For Ge-SCF, the conversion efficiency was below -31 dB and, as the effective length of Ge-SCF is more than 100 m, no component IL reduction was possible to enhance nonlinear performance. Further employment of Ge-SCF in the OPS was not considered. Evenmore when the pump peak power was at 16 dBm, Ge-SCF provided OSNR of switched data under 10 dB, which is below required values for typical optical communication. DFWM recorded spectra for Ge-PCF are illustrated in Fig. 6.

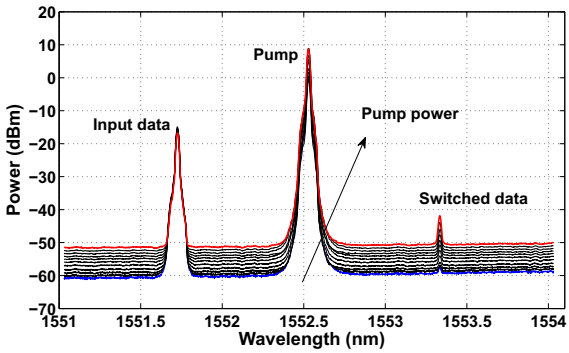

Fig. 6. Four-wave mixing in 100 m Ge-PCF, pump power from 6 dBm to 16 dBm.

Figure 7 then illustrates a comparison of all three NLFs and their conversion efficiencies. It can be observed that for pump peak powers over 12 dBm and 14 dBm for the HNLF and As_2Se_3 fiber respectively, SBS exhibits itself and starts to limit the conversion efficiency. In case of Ge-PCF the SBS treshold is still not trespassed. These results match the theoretical calculations.

4.1 Wavelength Range and Frequency Plan

With conversion efficiencies better than -15 dB at maximum pump peak power for HNLF with one channel detuning, additional measurements were carried out to evaluate conversion efficiency within wider wavelength range. In Fig. 8 conversion efficiency in dependence on channel detuning is presented with pump allocation at 1552.52 nm and with peak powers of 3 dBm, 8 dBm and 13 dBm. As can be observed flat conversion efficiency profiles were achieved

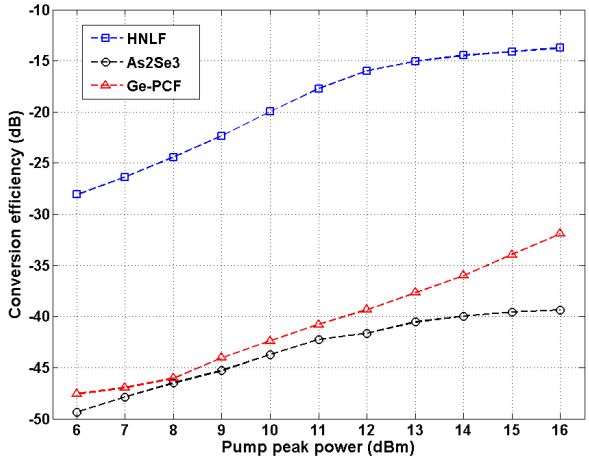

Fig. 7. Comparison of conversion efficiencies in dependence on pump peak power.

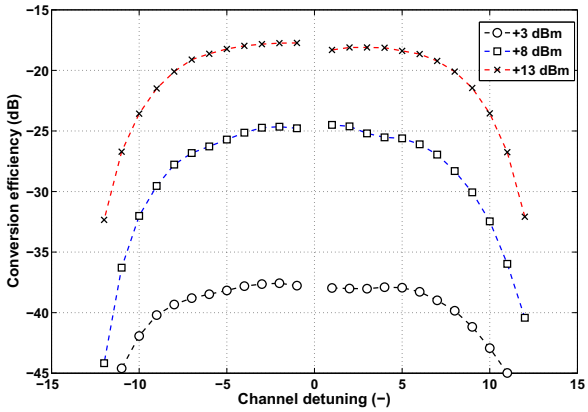

Fig. 8. HNLF - conversion efficiency in dependence on channel detuning and pump peak power, 100 GHz DWDM grid.

for ±8 channel detuning considering a 3 dB decrease limit, which is in perfect correlation with results published in [24]. The conversion efficiency increase between 8 dBm and 13 dBm pump was not as high as for 3 dBm to 8 dBm due to the onset of SBS.

For OPS based on DFWM it is significant to evaluate and decide for a spectrally efficient frequency plan. Attention was paid to facile filtering of the routing signals and input data, maximum conversion efficiency and frequency plan scalability. We considered a flat conversion profile of ±8 channels. The coarse frequency plan assumed routing signals (i.e. pumps) placed +3/+4 channels from the input data, switched data are then at +6/+8 channels from the former data signal for a 1x2 OPS. This setup enables utilization of commercially available filters (without requirement for filtering adjacent channels). If more outputs are required (1x4, 1x6 or 1x8 OPS), the setup can be expanded in a mirror-like fashion. Moreover in the dense option additional routing signals can be placed at +1/+5 channels, thus resulting in switched data at +2/+10 channels, but with significantly more complicated filtering or with higher requirements on AWG adjacent channel isolation than in the coarse variant.

4.2 BER and OSNR Tests

BER tests were performed to verify switching performance and to optimize the prototype subcomponents and cohesion between OEC and the optical part responsible for wavelength covnersion. A 10 Gbit/s NRZ (non-return zero) BER tester (BERT) was utilized as the input data source. As the pump source (Pump) a DFB diode was utilized. Polarization of both signals was controlled by polarization controllers (PCs) and coupled in a WDM multiplexer. Then both signals were amplified, where the total power booster (PB) output power varied from 10 dBm to 20 dBm, resulting as in previous measurements in 6 dBm to 16 dBm pump peak powers before HNLF. The polarization insensitive loop is described in detail in the following subsection. The switched signal was then filtered in an optical bandpass filter (OBF) to supress pump signal and former data signal and afterwards in AWG and amplified in a pre-amplifier (PRE-AMP). Finally the switched signal was detected at the BERT input. Complete setup is depicted in Fig. 9.

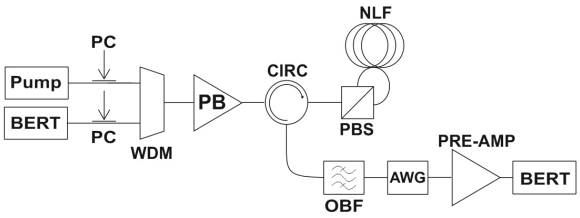

Fig. 9. Setup for OSNR, BER and polarization insensitivity measurements.

Obtained results are illustrated in Fig. 10, where the dependence of power booster total output power on BER is presented for HNLF. The best BER of 10^{-12} was achieved at 17 dBm, whereas for 16 dBm and 18 dBm BER values better than 10^{-10} were observed.

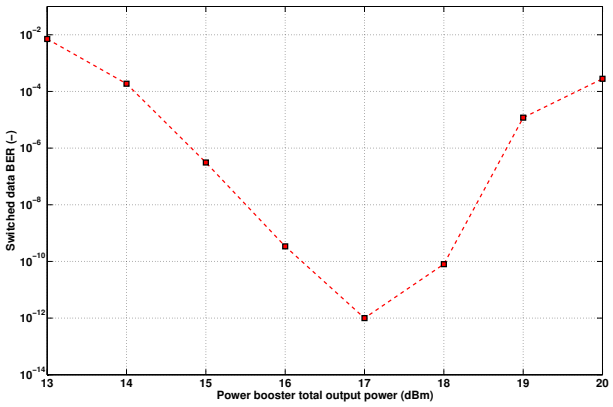

Fig. 10. Switched data BER dependence on the power booster total output power.

In Fig. 12 optical SNR (OSNR) and eye-diagram extinction ratio (ER) measuremend values of the switched signal are presented. Starting from 9 dBm pump peak powers, OSNR values exceeded 20 dB, but afterwards started to saturate around 25 dB with a decrease at 16 dBm pump peak power, i.e. 20 dBm power booster total output power, where ER was unmeasurable and also BER tests were lower than 10^{-4}.

This fact was accounted to high amplifier noise. The situation with best eye-diagram extinction ratio is presented in Fig. 11, with ER of 8.23 dB.

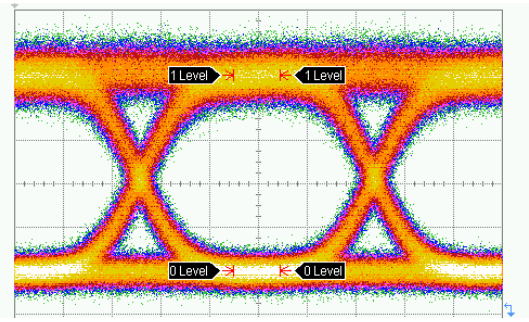

Fig. 11. Eye-diagram of the switched signal - extinction ratio of 8.23 dB.

From BER, OSNR and ER measurements, operation between 16 dBm to 18 dBm power booster total output power, i.e., pump peak power 12 dBm to 14 dBm, is desired. This is in good relation with previously calculated and measured SBS treshold.

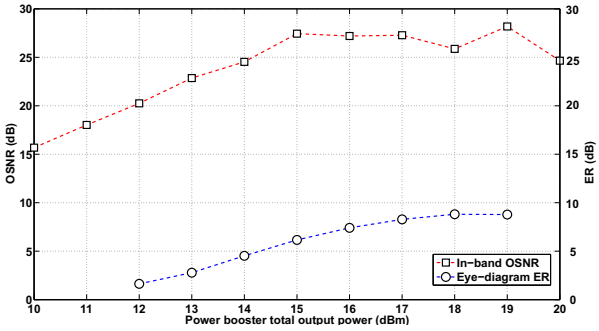

Fig. 12. Switched data in-band OSNR and eye-diagram ER for different power booster total output powers.

4.3 Polarization Insensitivity

For our polarization sensitivity measurements a setup incorporating an optical circulator (CIRC) and polarization beam-splitter (PBS) was selected. Setup of this configuration is identical to BER tests (see Fig. 9). The pump signal was coupled with the 10 Gbit/s NRZ signal from BERT. Then both input data and pump signal were amplified. NLF was placed in a loop and PBS divided the signals into fast and slow axes. The only critical condition was to keep the pump linear polarization in 45° to the slow axis of PBS, so that the pump power was equaly divided into the clockwise and counter-clockwise directions. Then the pump signal and input data were filtered (via OBF and AWG) and only switched data was detected at BERT.

In the experimental measurement power booster total output power was again tuned from 10 dBm to 20 dBm, resulting in 3 dBm to 13 dBm pump peak powers after PBS. By dividing the pump power, i.e. having two pumps with 3 dB lower peak powers, we operated closer to the SBS treshold in contrary to polarization sensitive configuration, where NLF was placed directly after power booster and in front of optical bandpass filter. The inclusion of CIRC and PBS resulted in only 0.5 dB insertion loss. Conversion efficiency difference between polarization sensitive (the best situation with co-polarized waves was considered) and insensitive variant at pump peak powers over 10 dBm was around 3 dB. Polarization state of the input data was then varied in a 90° range with maximal difference in conversion efficiency of ±0.6 dB. Tuning the pump polarization state from the optimal 45° by less than 10° resulted only in insignificant variations of the output idler power. When the state of polarization was varied in the polarization sensitive setup, the switched data peak power values decreased rapidly.

5. Simulations

For additional comparison, simulations were carried out in Optiwave Optisystem software. Further polarisation features tested via simulation are presented in Fig. 13. For the polarization insensitive variant (blue) only small fluctuations of switched data peak power are observed (∼0.01 dB). In case of the polarization sensitive setup (red), when the input data polarization state is tuned from +0° to +90° from the pump polarization state, almost 16 dB decrease in switched data peak power level is present.

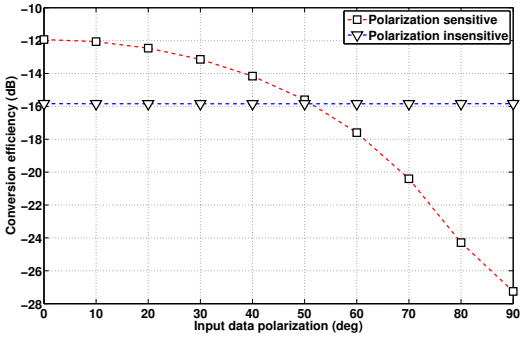

Fig. 13. Simulated switched data conversion efficiency in HNLF, when input data polarization is tuned by +0° to +90° with respect to the pump signal.

5.1 As_2Se_3 Fiber Optimization

Following As_2Se_3 fiber connectorization technology development, parameter characterization and primary conversion efficiency measurement further optimization was necessary. The component IL of 16.0 dB could be significantly reduced if only the effective length is utilized, which was calculated as 7.5 m for the employed As_2Se_3 fiber. Thus it was possible to decrease component IL to 4.9 dB, while maintaining the same nonlinear response. Conversion efficiency increased to -16.1 dB where the results were obtained within simulations considering a 5 m long As_2Se_3 fiber. Further analysis of As_2Se_3 fiber length in range from 1 m to 10 m suggests, that with employment of 3 m to 6 m long As_2Se_3 fiber segment, maximized switched data peak powers are obtained. Considering the aim of broadest wavelength range for the data switching, it is suitable to utilize

As_2Se_3 fiber segment of the shortest length, thus eliminating the effects of dispersion induced walk-off. Conversion efficiencies for different As_2Se_3 fiber lengths are presented in Fig. 14. In comparison with [7], we have demonstrated comparable conversion efficiencies to HNLF for As_2Se_3 fiber lengths of several meters, enabling employment of such components in the OPS prototype.

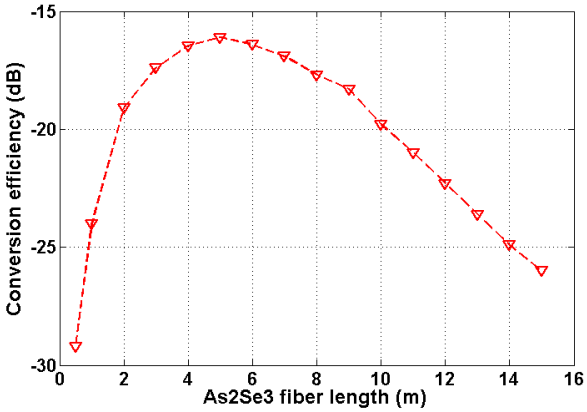

Fig. 14. Simulated switched data conversion efficiency in As_2Se_3 fiber with respect to fiber length.

6. Conclusion

Development of a data transparent and polarization insensitive optical packet switch prototype based on fibers with enhanced nonlinearity was presented. Technology of chalcogenide glass fiber processing and connectorization has been perfected. A single-mode arsenic-selenide fiber with cut-off at 1300 nm was connectorized and a component with 26 m length was developed. Attenuation of 0.6 dB/m was measured with connection losses of 0.25 dB to conventional silica fiber, thus presenting enhancement of current state-of-art parameters. Ge-doped suspended-core silica microstructured fiber by IPHT, Jena, Germany was also connectorized, providing connection loss of 0.9 dB.

Conversion efficiencies were measured for all utilized fibers. HNLF provided conversion efficiency of almost -13 dB. Conversion efficiency for the As_2Se_3 fiber was below -38 dB due to component insertion loss of 16 dB. Optimization within simulations with shorter lengths of As_2Se_3 fiber was carried out, where 5 m of As_2Se_3 fiber provided conversion efficiency of -16 dB. Ge-SCF showed almost no nonlinear response with conversion efficiency below -38 dB.

HNLF was employed for experimental optical packet switching, with modulation format transparent switching, sixteen 100 GHz DWDM channels flat conversion efficiency profile and polarization insensitive operation in the final proposed switching configuration. On the other hand SBS treshholds for HNLF were the lowest of all utilized fibers with enhanced nonlinearity. BER tests were performed for the polarization insensitive configuration with extinction ratio of more than 8 dB for the best eye-diagrams. BER better than 10^{-10} was observed. In-band OSNR measurements better than 25 dB were observed.

The introduced device follows amplification constrains given by long haul optical networks and combines good conversion efficiency with negligible polarization dependence. Functionality was tested and verified on HNLF, where simulations results imply significant enhancement in the device parameters, by employing the optimized As_2Se_3 fiber. Technical details have been protected under an utility model and in an ongoing patent process.

Acknowledgements

The authors thank SQS Fiber optics, Czech Republic for support and cooperation in the development of technological processes of chalcogenide fibers and IPHT Jena, Germany for providing the Ge-doped microstructured fiber under the framework COST Action TD1001. Furthermore we thank Petr Dvorak for his help with the development of the processing unit. This work was supported by the CTU grant No. SGS14/190/OHK3/3T/13.

References

[1] TIPSUWANNAKUL, E., LI, J., KARLSSON, M., ANDREKSON, P., Performance comparisons of DP-16QAM and duobinary-shaped DP-QPSK for optical systems with 4.1 bit/s/Hz spectral efficiency. *Journal of Lightwave Technology*, 2012, vol. 30, no. 14, p. 2307 - 2314.

[2] NAKAZAWA, M., OKAMOTO, S., OMIYA, T., KASAI, K., YOSHIDA, M., 256-QAM (64 Gb/s) coherent optical transmission over 160 km with an optical bandwidth of 5.4 GHz. *IEEE Photonics Technology Letters*, 2010, vol. 22, no. 3, p. 185 - 187.

[3] CALABRETTA, N., WANG, G., DITEWIG, T., RAZ, O., AGIS, F., DE WAARDT, S., DORREN, H. Scalable optical packet switches for multiple data formats and data rates packets. *IEEE Photonics Technology Letters*, 2010, vol. 22, no. 7, p. 483 - 485.

[4] HUYBRECHTS, K., MORTHIER, G., BAETS, R. Fast all-optical flip-flop based on a single distributed feedback laser diode. *Optics Express*, 2008, vol. 16, no. 15, p. 11405 - 11410.

[5] CHOU, H. F., HUANG, C.-H., BOWERS, J., TOUDEH-FALLAH, F., GUYREK, R. 3-D MEMS-based dynamically reconfigurable optical packet switch (DROPS). In *Proceedings of the International Conference on Photonics in Switching*. 2006, p. 1 - 3.

[6] LUO, J., DORREN, H. J. S., CALABRETTA, N. Optical RF tone in-band labeling for large-scale and low- latency optical packet switches. *Journal of Lightwave Technology*, 2012, vol. 30, no. 16, p. 2637 - 2645.

[7] NAKANISHI, T., HIRANO, M., OKUNO, T., ONISHI, M. Silica-based highly nonlinear fiber with g =30/W/km and its FWM-based conversion efficiency. In *Proceedings of the Optical Fiber Communication Conference and Exposition and The National Fiber Optic Engineers Conference.* Anaheim (CA, USA), 2006, p. OTuH7.

[8] SANGHERA, J. S., SHAW, L. B., PUREZA, P., NGUYEN, V. Q., GIBSON, D., BUSSE, L., AGGARWAL, I. D., FLOREA, C. M., KUNG, F. H. Nonlinear properties of chalcogenide glass fiber. *International Journal of Applied Glass Science*, 2010, vol. 1, no. 3, p. 296 - 308.

[9] CHANG, Y.-M., LEE, J., LEE, J. H. Bismuth nonlinear optical fiber for photonic ultrawideband radio- signal processing. *IEEE Journal of Selected Topics in Quantum Electronics*, 2012, vol. 18, no. 2, p. 891 - 898.

[10] FENG, X., POLETTI, F., CAMERLINGO, A., PARMIGIANI, F., PETROPOULOS, P., HORAK, P., PONZO, G. M., PETROVICH, M., SHI, J., LOH, W. H., RICHARDSON, D. J. Dispersion controlled highly nonlinear fibers for all-optical processing at telecoms wavelengths. *Optical Fiber Technology*, 2010, vol. 16, no. 6, p. 378 - 391.

[11] LE, S. D., NGUYEN, D. M., THUAL, M., BRAMERIE, L., SILVA, M. C., LENGLÉ, K., GAY, M., CHARTIER, T., BRILLAND, L., MÉCHIN, D., TOUPIN, P., TROLES, J. Efficient four-wave mixing in an ultra-highly nonlinear suspended-core chalcogenide As38Se62 fiber. *Optics Express*, 2011, vol. 19, no. 26, p. B653 - B660.

[12] SANGHERA, J., SHAW, L. B., PUREZA, P., NGUYEN, V. Q., GIBSON, D., AGGARWAL, I. D., FLOREA, C. M., KUNG, F. Progress of chalcogenide glass fibers. In *Proceedings of the Optical Fiber Communication Conference and Exposition and The National Fiber Optic Engineers Conference*. Anaheim (CA, USA), 2007, p. 1 - 3.

[13] TAEED, V. G., FU, L., PELUSI, M., ROCHETTE, M., LITTLER, I. C., MOSS, D. J., EGGLETON, B. J. Error free all optical wavelength conversion in highly nonlinear As-Se chalcogenide glass fiber. *Optics Express*, 2006, vol. 14, no. 22, p. 10371 - 10376.

[14] TOROUNIDIS, T. *Fiber Optic Parametric Amplifiers in Single and Multi Wavelength Applications.* PhD thesis. Gothenburg (Sweden): Chalmers University of Technology, 2006.

[15] DONG, L., THOMAS, B. K., FU, L. Highly nonlinear silica suspended core fibers. *Optics Express*, 2008, vol. 16, no. 21, p. 16423 - 16430.

[16] MAGI, E., YEOM, D.-I., NGUYEN, H., FU, L., EGGLETON, B. Enhanced Kerr nonlinearity in sub-wavelength diameter As2Se3 chalcogenide fibre tapers. In *Proceedings of the Optical Internet 2007 and the 2007 32nd Australian Conference on Optical Fibre Technology (COIN-ACOFT).* Melbourne (Australia), 2007, p. 1 - 3.

[17] *IEEE Standard for Information technology- Telecommunications and information exchange between systems-Local and metropolitan area networks- Specific requirements Part 3: Carrier Sense Multiple Access with Collision Detection (CSMA/CD) Access Method and Physical Layer Specifications Amendment 4: Media Access Control Parameters, Physical Layers and Management Parameters for 10 Gb/s Operation*. IEEE Std 802.3ae. IEEE, 2002.

[18] *IEEE Standard for Information technology- Telecommunications and information exchange between systems-Local and metropolitan area networks- Specific requirements Part 3: Carrier Sense Multiple Access with Collision Detection (CSMA/CD) Access Method and Physical Layer Specifications Amendment 4: Media Access Control Parameters, Physical Layersand Management Parameters for 40 Gb/s and 100 Gb/s Operation*. IEEE Std 802.3ba. IEEE, 2010.

[19] YU, C., PAN, Z., WANG, Y., SONG, Y., GURKAN, D., HAUER, M., WILLNER, A., STARODUBOV, D. Polarization insensitive four-wave mixing wavelength conversion using a fiber Bragg grating and a Faraday rotator mirror. In *Proceedings of the Optical Fiber Communications Conference (OFC).* 2003, p. 347 - 349.

[20] SAKAMOTO, T., SEO, K., TAIRA, K., MOON, N. S., KIKUCHI, K. Polarization-insensitive all-optical time division demultiplexing using a fiber four-wave mixer with a peak-holding optical phase-locked loop. *IEEE Photonics Technology Letters*, 2004, vol. 16, no. 2, p. 563 - 565.

[21] HU, H., MULVAD, H., GALILI, M., PALUSHANI, E., XU, J., CLAUSSEN, A., OXENLOWE, L., JEPPESEN, P. Polarization-insensitive 640 Gb/s demultiplexing based on four wave mixing in a polarization-maintaining fibre loop. *Journal of Lightwave Technology*, 2010, vol. 28, no. 12, p. 1789 - 1795.

[22] MOSSADEGH, R., SANGHERA, J. S., SCHAAFSMA, D., COLE, B. J., NGUYEN, V. Q., MIKLOS, R. E., AGGARWAL, I. D. Fabrication of single-mode chalcogenide optical fiber. *Journal of Lightwave Technology*, 1998, vol. 16, no. 2, p. 214.

[23] ELSCHNER, R., BUNGE, C. A., HUTTL, B., I COCA, A., SCHMIDT-LANGHORST, C., LUDWIG, R., SCHUBERT, C., PETERMANN, K. Impact of pump-phase modulation on FWM-based wavelength conversion of D(Q)PSK signals. *IEEE Selected Topics in Quantum Electronics*, 2008, vol. 14, no. 3, p. 666 - 673.

[24] ONISHI, M., OKUNO, T., KASHIWADA, T., ISHIKAWA, S., AKASAKA, N., NISHIMURA, M. Highly nonlinear dispersion-shifted fibers and their application to broadband wavelength converter. *Optical Fiber Technology*, 1998, vol. 4, no. 2, p. 204 - 214.

About Authors ...

Matej KOMANEC was born in 1984. He received MSc. and Ph.D. degrees from the Faculty of Electrical Engineering of the Czech Technical University in Prague where he is now a research employee. His professional interests cover fiber optics, nonlinear phenomena, specialty fibers and fiber sensing.

Pavel SKODA was born in 1982. He received MSc. degree from the Faculty of Electrical Engineering of the Czech Technical University in Prague where he is now a research employee. His professional interests cover optical fiber communication, all-optical networks, modulation formats and all-optical devices.

Jan SISTEK was born in 1974. He received MSc. and Ph.D. degrees from the Faculty of Electrical Engineering of the Czech Technical University in Prague where he is now an Assistant Professor. His professional interests cover optical fibers and associated electronics, microwave circuits and related measurement techniques.

Tomas MARTAN was born in 1976. He received MSc. and Ph.D. degrees at the Faculty of Electrical Engineering of the Czech Technical University in Prague where he is now an Assistant Professor. His professional interests cover specialty fibers, optical fiber sensing, optoelectronics and optical spectroscopy.